DEPARTMENT OF
MINERALS AND ENERGY

BUREAU OF MINERAL RESOURCES,
GEOLOGY AND GEOPHYSICS

Record 1975/30

GEOLOGICAL WORK IN ANTARCTICA - 1974

by

R.N. England & A.P. Langworthy

Record 1975/30

GEOLOGICAL WORK IN ANTARCTICA - 1974

by

R.N. England & A.P. Langworthy

CONTENTS

PLATES (Contd.)

FIGURES

FIGURES (Contd.)

SUMMARY

Four localities in the southern Prince Charles Mountains, and a small Nunatak west of the Grove Mountains, were visited during the summer of 1974. The rocks of the southern end of the Mawson Escarpment and probably those of Mounts Rubin and Ruker belong to a comparatively young east-west belt characterized by high-pressure facies, culminating in kyanite-staurolite-grade metamorphism. Mount Newton, to the south of the east-west belt, consists of older basement rocks, and Austin Nunatak, west of the Grove Mountains, is composed of rock probably equivalent to the basement in the Prince Charles Mountains. Rb/Sr dating suggests that both basement and cover rocks are of late Archaean age.

A miogeosynclinal sequence overlying older granite at Mount Ruker contains stratiform iron ore deposits which are similar to both the Archaean and Proterozoic iron formations of Western Australia. The sequence includes quartzite, volcanics, dolomitic schist, black slate, and greywacke. The iron formations, which occur at a number of stratigraphic levels, are low grade; very few samples exceed 35 percent iron. Although folding is not evident on a large scale, tight mesoscopic and microscopic folds are common.

At Mount Rubin an unsuccessful search for Cambrian fossils was made and some details of the structure recorded. At Mount Newton upper amphibolite facies basement rocks have been partly retrogressed, probably during the same event which has progressively metamorphosed the younger rocks. The structure is simple and little folding is associated with the retrogressive phase of deformation.

Old high-grade metasediments and leucogneisses in the southern Mawson Escarpment have been markedly retrogressed in the low amphibolite facies metamorphism which affected the younger belt. In many rocks over-printing has been strong enough to mask almost all the features inherited from the earlier high grade metamorphism. Some rocks have no original features preserved and may, in fact, belong to the younger east-west belt.

Quartz-rich gneisses with calc-silicate affinities form the bulk of the outcrop at Austin Nunatak. Pegmatite, and interlayered calc-silicate and microcline-rich gneisses also occur there.

INTRODUCTION AND GEOLOGICAL SETTING

Semidetailed geological work was carried out from 5-27 January 1974 in areas of special interest selected after the wide-ranging aerial reconnaissance of 1973. The areas chosen for semidetailed work, which was done with very limited aerial support, were: the Mount Ruker iron ore deposits, northern Mount Newton, the southern Mawson Escarpment, Mount Rubin, the northern Mawson Escarpment, and as many localities as possible in the Grove Mountains. It was not possible to visit the two last areas because of the failure of the latter half of the 1974 summer program. Locations visited are shown in Fig. 1.

The rocks of the Prince Charles Mountains form part of the east Antarctic Precambrian shield. With minor exceptions they are strongly metamorphosed, although the metamorphic grade in the southern Prince Charles Mountains is generally lower than in nearby areas in east Antarctica. The intensity of metamorphism in the southern Prince Charles Mountains ranges from biotite grade at Mounts Rubin, Ruker, and Seddon, to lower granulite facies in the northern part of the Mawson Escarpment. A broad east-west belt of lower amphibolite facies rocks extending from Mount Menzies to the south Mawson Escarpment is 'sandwiched' between higher-grade rocks to the north and south. The central part of the lower-grade belt contains the weakly metamorphosed rocks of Mounts Rubin, Ruker, and Seddon. The structural trends in the low-grade and high-grade rocks are east-west. Although the east-west belt of lower-grade rocks appears, in general, to be younger than the high-grade rocks on either side, some rocks in the belt retain features of an earlier higher-grade metamorphism and appear to be representatives of the older higher-grade terrain that have been incorporated into the younger belt during orogenesis. Rocks with well-preserved sedimentary structures, unlikely to have gone through an early high-grade metamorphism, are characteristic of the low-grade belt. Retrograde metamorphism has affected almost all of the high-grade rocks, more particularly those close to the lower-grade belt.

In the south Mawson Escarpment and at Mount Newton, high-grade older rocks have been markedly retrogressed during the later staurolite-grade event which affected the younger belt. Austin Nunatak, 25 km west of the Grove Mountains, consists mainly of siliceous gneiss with calc-silicate affinities which resemble rocks at Wilson Bluff, and Mounts Twigg and Borland which probably belong to the Prince Charles Mountains basement complex.

THE GEOLOGY OF THE CENTRAL PART OF MOUNT RUKER (CUMPSTON MASSIF SHEET AREA, SS40-42/7)

Mount Ruker is divided by a large central north-facing embayment which is filled with stagnant ice and moraine. A geological reconnaissance was made from a camp site on the platform to the east of the embayment, and another at the base of the cliffs immediately to the west of it. A geological map, Figure 2, is included.

The platform on the eastern side is covered with a felsenmeer of more or less in situ frost-wedged rubble. No outcrop occurs in this part of the area, but the outline of the underlying rock types can be observed in the felsenmeer. In the northeast part of the area, and extending across the whole of the northeast part of the mountain, is a biotite granite consisting of quartz, microcline, saussuritized and sericitized sodic plagioclase, secondary carbonate, and secondary biotite. The granite is intruded by numerous basic dykes with greenschist facies assemblages - typically containing actinolite, albite, epidote, and chlorite, with minor biotite and sphene.

Low grade miogeosynclinal metasediments which include a number of jaspilite horizons outcrop to the southwest of the granite. The boundary between the granite and metasediments is roughly parallel to the strike of the latter. Basic dykes intrude only the granite and some appear to be truncated at the granite-metasediment boundary. No pegmatitie or aplite

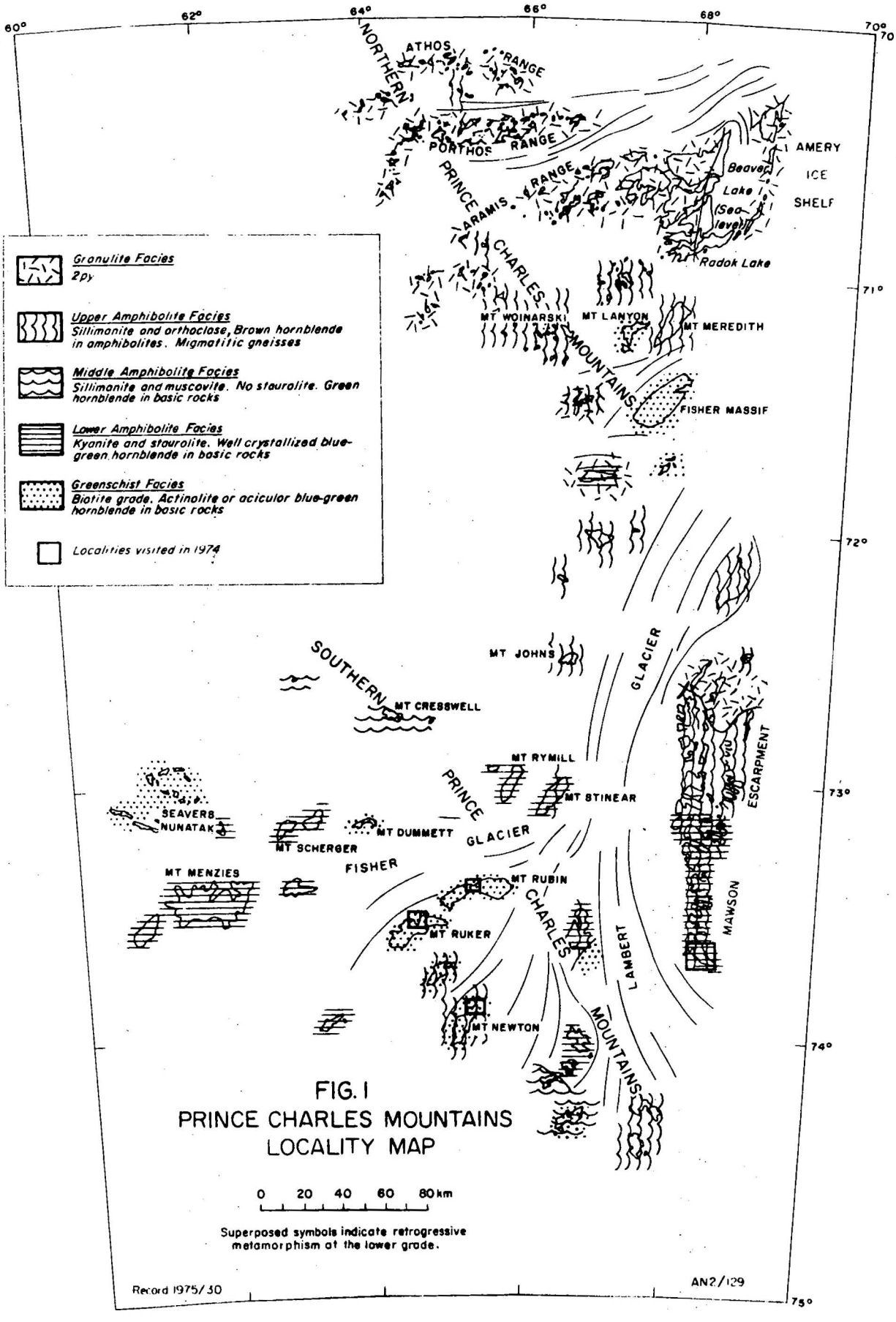

FIG. 1
PRINCE CHARLES MOUNTAINS
LOCALITY MAP

Fig.2-Geological sketch map of the central part of Mount Ruker

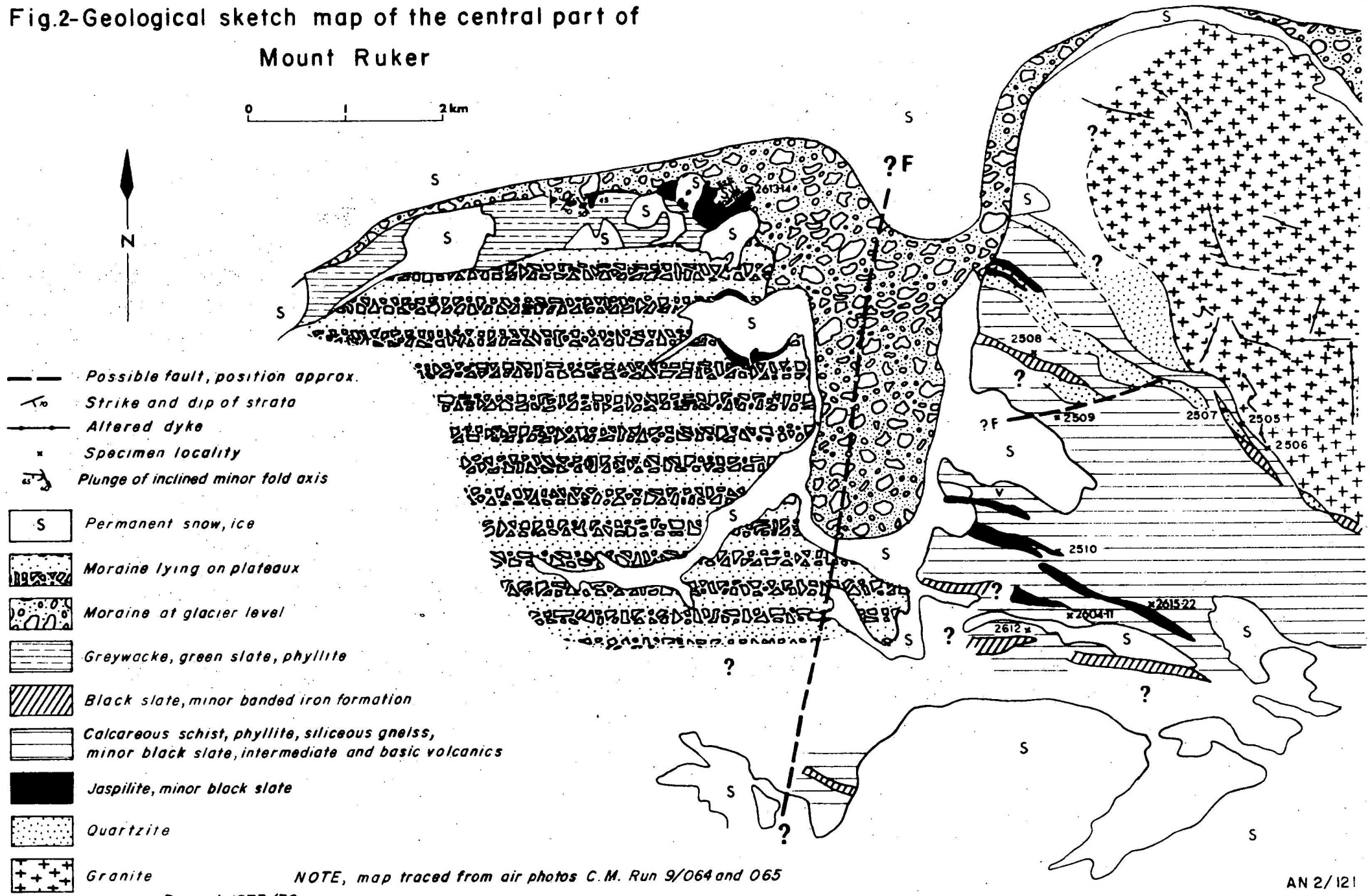

NOTE, map traced from air photos C.M. Run 9/064 and 065

Record 1975/30

AN 2/121

dykes, or contact metamorphic effects, have been observed in the metasediments, and it is concluded that they overlie the granite unconformably. A broad quartzite unit near the northwestern end of the granite-metasediment boundary appears to be truncated abruptly at its contact with the granite; such a feature may, however, have resulted from valley fill in an old erosion surface.

The lack of outcrop makes the dip of the metasediments difficult to estimate, but the slope of the boundary between quartzite and jaspilite on the moderately steep escarpment shown in Plate 1 suggests that there, at least, the dip is nearly vertical. Pure white and limonite-stained orange quartzites with polygonal quartz grains are common near the granite. In places they are stained green with fuchsitic? mica characteristic of similar rocks from Mounts Stinear, Menzies, and Rymill. Interlayered with the quartzites, and dominant among the rocks above them, is a sequence of chlorite-white mica-quartz schists, green chlorite phyllites, dolomite-rich chlorite schists, coarse grained highly siliceous rocks, black chlorite-carbonate-actinolite-biotite slates, jaspilites, metamorphosed basic and fine-grained porphyritic andesitic volcanic rocks, and minor talc-carbonate rocks. There appears to be a complete gradation between black slate and jaspilite. The jaspilite is tightly folded on a mesoscopic and microscopic scale but no folding occurs on a macroscopic scale. Clastic ironstones are very rare; the only example discovered was a piece of rubble composed of sedimentary breccia of jaspilite fragments up to 4 cm across. A typical jaspilite (74282510) contains magnetite (about 20%), moderately fine polygonal-grained quartz (about 60%), carbonate (about 15%), and dark brown biotite. Sample 73281699, from a jaspilite bed near the bottom of the sequence contains less magnetite, but considerable amounts of very fine-grained garnet. The presence of abundant garnet in rocks of such low metamorphic grade suggests that they are rich in manganese.

To the west of the large embayment, the pattern of the geology is not clear. Most of the plateau areas are covered with thick moraine, although outcrops of jaspilite occur along the flanks of a small glacier which feeds the embayment from the west. Only on the north-facing cliffs to the west of the embayment are there extensive outcrops. Jaspilite, (first described by Soloviev (1972), outcrops at the eastern end of the cliffs. Four smaller outcrops of iron formation occur on the headlands for about 1 km to the west of the main body of jaspilite.

Structure

The main body of jaspilite outcrops over about 750 m of cliff face; its visible thickness is about 750 m thick, but its true thickness may be less. The bottom of the unit is buried beneath the glacier. The cliff forms an approximate cross-section of the folds, giving an undistorted impression of fold style.

Open concentric and highly flattened mesoscopic folds are ubiquitous within the jaspilite formation. Folds are slightly curviplanar and cylindrical. The dip of axial planes (about 65° towards 240°) and the plunge (about 40° towards 190°) remain fairly constant over the whole outcrop.

Figure 3 shows the orientation of the structural elements of the jaspilite outcrop. The plunge of the folds is very nearly parallel to the contact with the overlying greywacke, but their axial planes lie at an oblique angle to the boundary between the two rock units. Layering in the jaspilite near the contact is parallel to the lithological boundary and is not folded.

PLATE 1. Mount Ruker. Almost vertically dipping interbedded jaspilites, black slates, basic volcanics (all dark), and quartzite (light) on the eastern side of the large north-facing embayment. Quartzite bed is about 100 m thick. Note tide mark of till composed largely of quartzo-feldspathic gneiss.

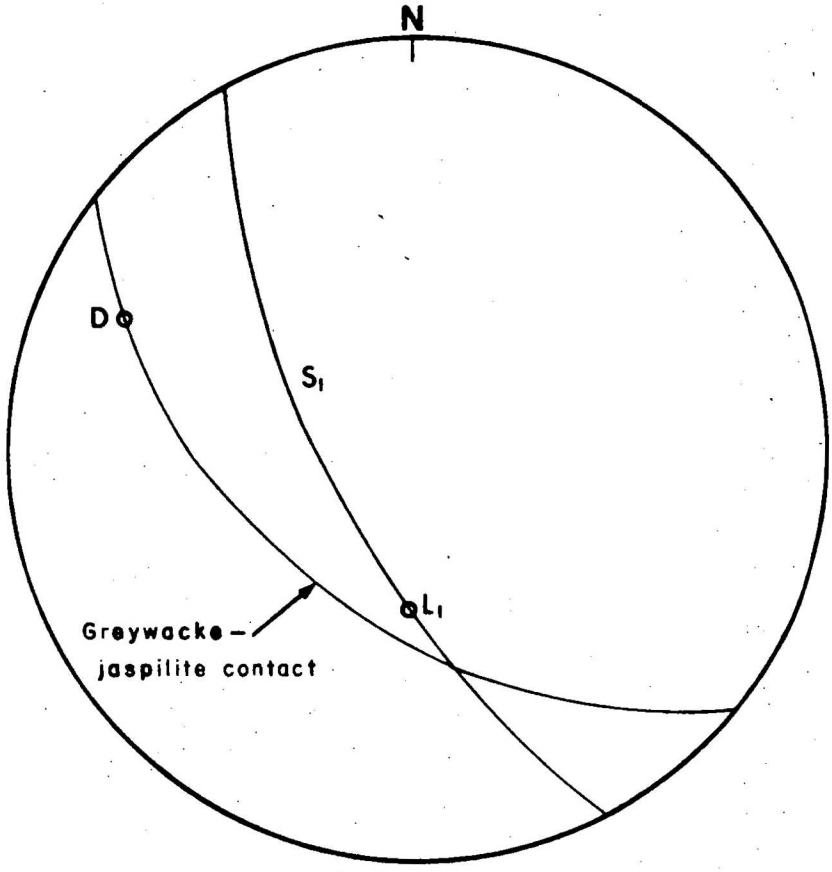

Fig. 3. Orientation of structural elements in the Mount Ruker jaspilite outcrop. S_1 = axial plane of mesoscopic folds. L_1 = axes of mesoscopic folds. Note that L_1 is very nearly parallel to the greywacke–jaspilite contact. D, the suggested direction of shear, lies in the plane of the greywacke–jaspilite contact and is normal to L_1.

PLATE 2. Mount Ruker, west of the north-facing embayment. Jaspilite beds outcropping on headlands and dipping to the right (south) under a monotonous sequence of grey-green slate and greywacke.

PLATE 3. Mount Ruker. Thick moraine field perched at plateau level 500 m above the present ice level.

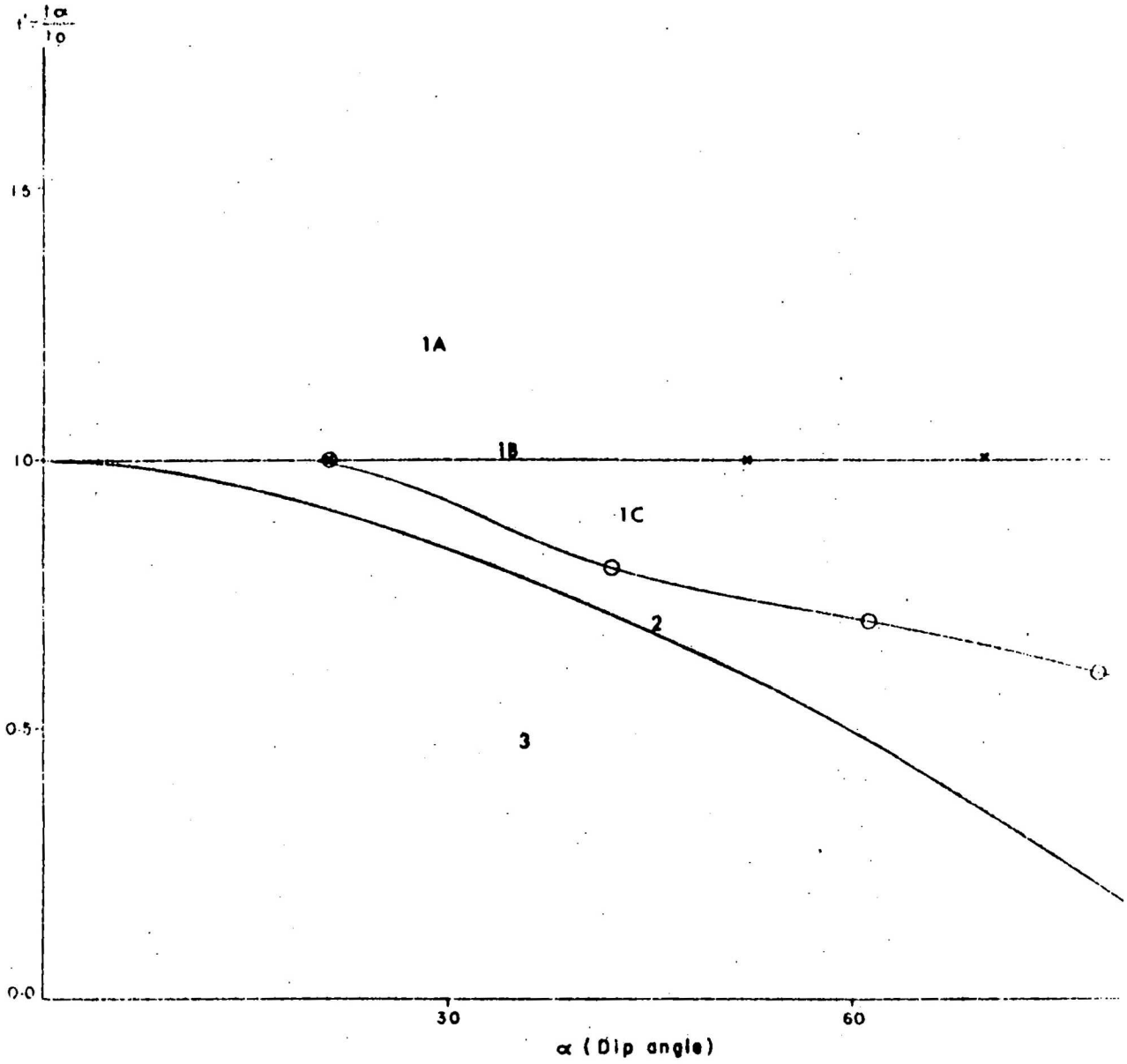

Fold 1 × Class 1B (Plate 5)
Fold 2 O Class 1C (Plate 6)

Fig.4 - Thickness analysis of parallel and highly flattened folds in Mt. Ruker jaspilite

AN2/123

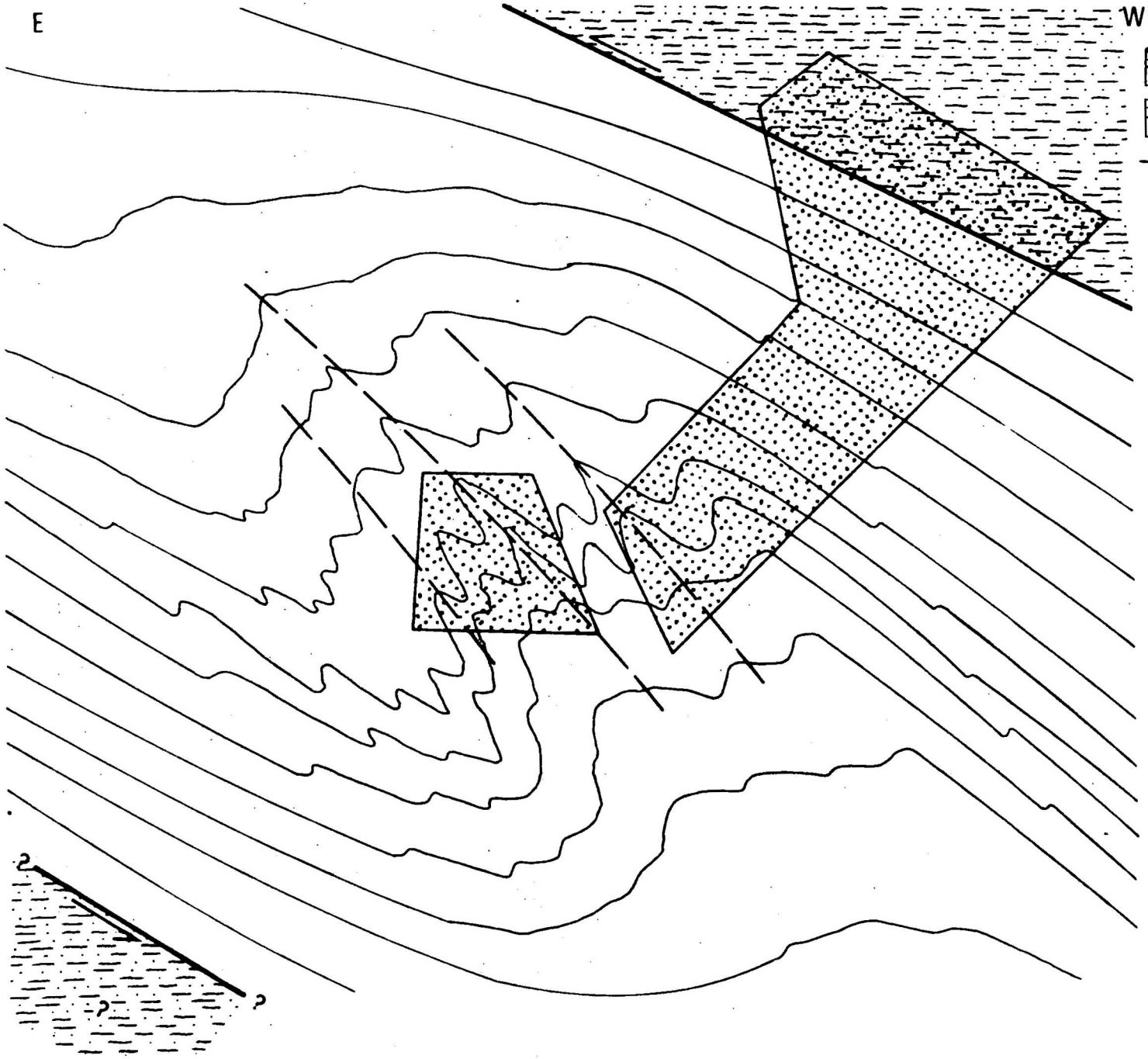

Fig. 5. Suggested model for deformation at the Mount Ruker jaspilite outcrop. Section is roughly parallel to the cliff face and also normal to the fold axes which plunge at about 45° due south. Fold axes are nearly parallel to the plane of contact of greywacke and jaspilite. Only the stippled area represents outcrop; the rest of the diagram is hypothetical. Arrows indicate the possible sense of shearing.

To accompany Record 1975·30

AN 2/124

Table 1. The structural elements recognized in the Mount Ruker jaspilite outcrops.

Symbol	Fabric Element	Relationship
S_0	Compositional layering in banded iron formation; almost certainly identical with bedding	Folded by F_1
S_1	Foliation parallel to axial planes of F_1 folds. Observed only rarely. In some samples - riebeckite needles are distributed randomly in S_1. In places minor crenulation cleavage developed in jaspilite. Schistosity in rare calcareous schists within the jaspilite sequence (Plate 11)	
L_1	Preferred orientation of riebeckite needles developed in some samples of tightly folded jaspilite. Parallel with axes of mesoscopic and microscopic folds	
F_1	Slightly curviplanar cylindrical folds in S_0. Concentric folds modified by flattening	

Fold style. The folds in the jaspilite outcrops studied fall into three groups according to scale. The style of the folds can be classified quantitatively using the method of Ramsay (1967). The ratio (A') of orthogonal thickness at a given point (t_α) to the orthogonal thickness at the nose (t) is plotted against the angle (α) between the tangent at that point and the tangent at the nose for a number of points on the fold. α is called the dip angle in Fig 4. All folds measured occur in the siliceous lamellae.

(i) The largest mesoscopic folds have an open concentric style with wavelengths of about 12-25 m and amplitudes of about 6-10 m. Most of these folds are symmetrical, of the flexural slip type, and fall into Ramsay's Class 1B.

(ii) On the limbs of the large scale folds are parasitic, harmonic, highly flattened, asymmetrical buckle folds (Plate 6) with wave-lengths of 2 to 3 m and amplitudes of about 2 m. They are generally of a similar style and approximate Ramsay's Class 1C (see Fig. 4).

(iii) Small, disharmonic, irregular, asymmetrical folds (Plate 5) occur in the hinge regions of the highly flattened folds. Here, 2-3 cm thick siliceous layers lying in incompetent ironstone have been buckled into Class 1B folds (Plate 5, Fig. 4). They are usually open but cuspate forms occur in places.

In regions where the siliceous lamellae are thin, the folds in the ironstone resemble the similar model (Class 2), whereas those in the siliceous lamellae are chevron folds of the concentric type with straight limbs and tight noses (Plate 7).

PLATE 4. Mount Ruker. Concentric folding in the jaspilites shown in Plate 2.

PLATE 5. Mount Ruker. Parallel Class 1B fold in siliceous layer.

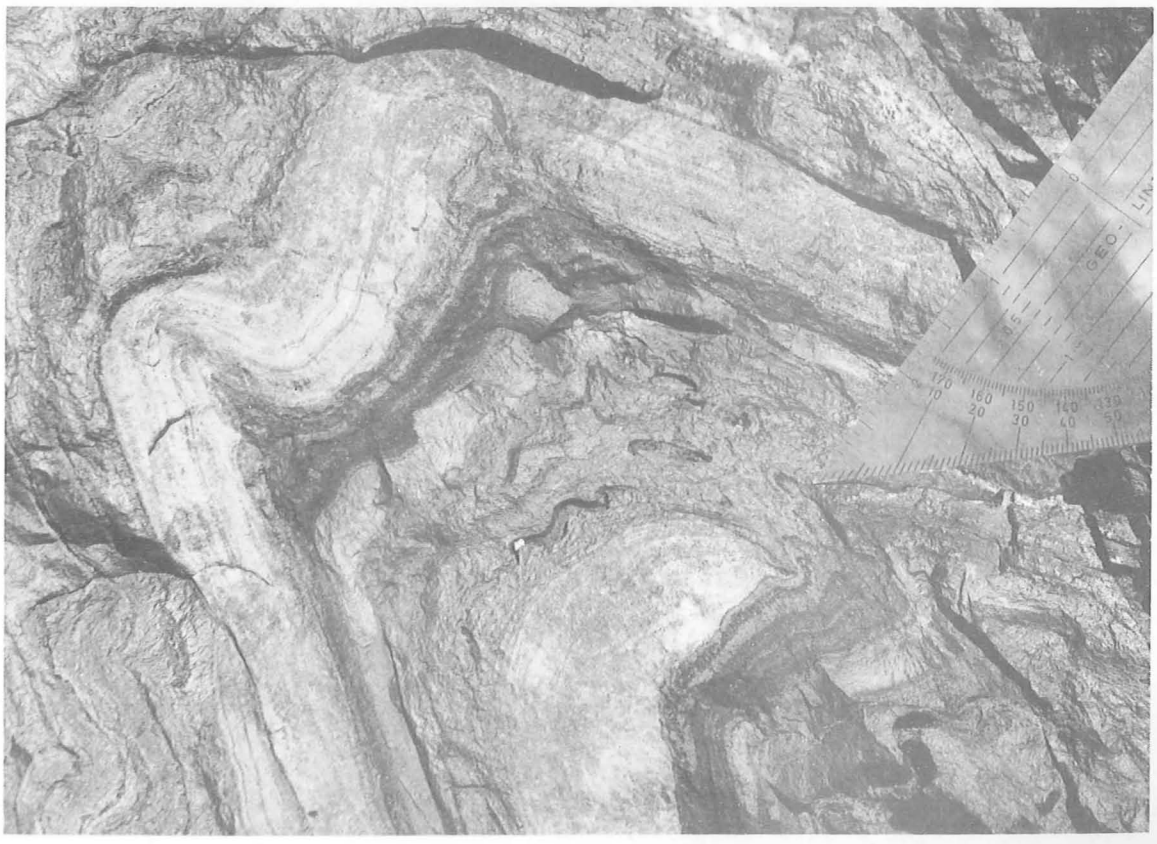

PLATE 6. Mount Ruker. Highly flattened concentric folds

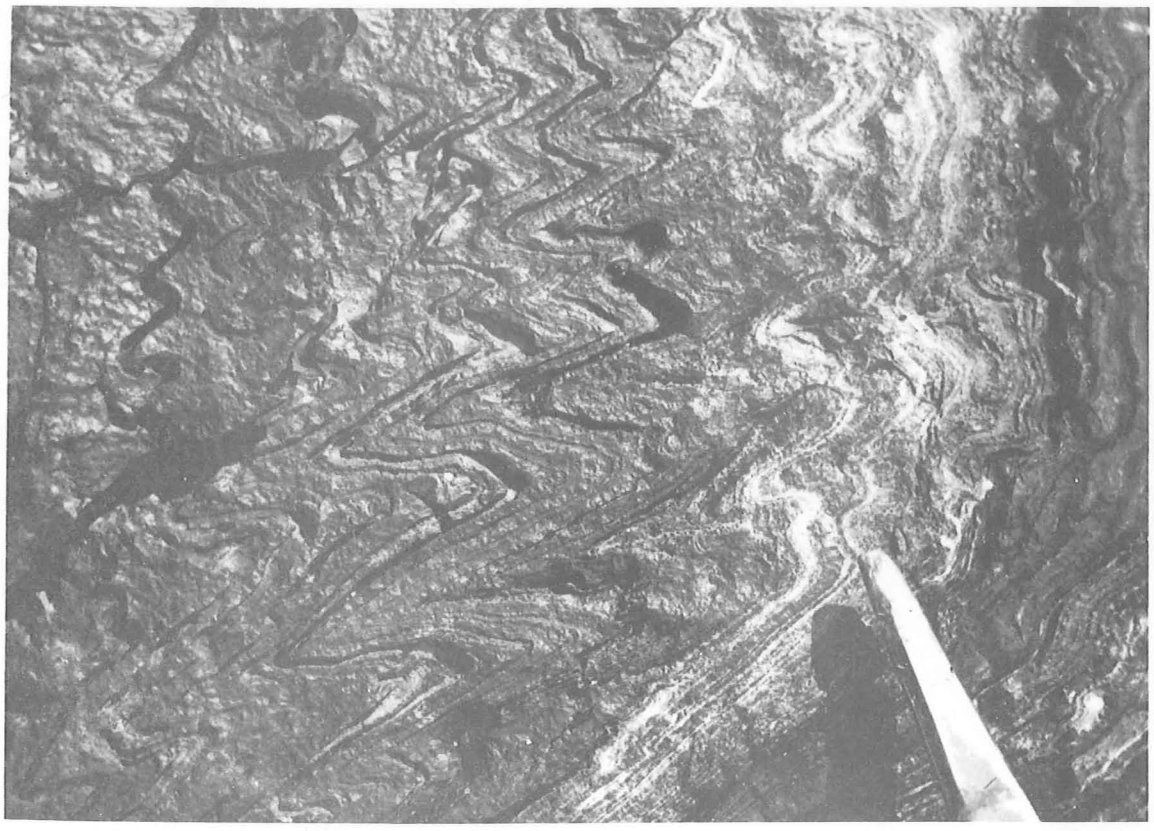

PLATE 7. Mount Ruker. Small scale chevron folds in thinly banded siliceous lamellae.

In places, buckled siliceous lamellae have been flattened (Plate 8, Fig. 4), disrupted (Plate 9), and attenuated. At some localities decollement which has occurred along ferruginous layers is associated with half-wave buckling of thin siliceous layers (Plate 10).

Petrofabric. The jaspilite consists of alternating siliceous and ferruginous layers. Siliceous layers consist largely of fine-grained aggregates of allotriomorphic quartz grains. Heavily sutured grain boundaries are evident in some rocks. Ferromagnesian silicates such as riebeckite, stilpnomelane, biotite, and possible minnesotaite occur in distinct lamellae, parallel with and close to the boundary between siliceous and ferruginous layers. The latter are composed of magnetite grains, mostly with an octahedral or distorted octahedral habit, in a matrix of quartz, minor ferromagnesian minerals, and carbonate. Even the most iron-rich specimens probably contain only about 35 percent magnetite by volume giving them a maximum iron content of about 35 weight percent. Individual lamellae of both types range from 1 mm to several centimetres in thickness. In some specimens riebeckite needles have a preferred orientation parallel to the hinges of tight microfolds. In others, the needles tend to be randomly orientated within the axial planes of the microscopic and mesoscopic folds.

Structural interpretation. It is evident that the dominant mechanism of folding was simple buckling of highly competent multiple layers of siliceous material, with flow of the interlaminated ferruginous material to accommodate itself to the fold forms imposed by the buckled siliceous layers. A certain amount of flattening near the noses of tight folds in the siliceous layers is probably the result of a high degree of lateral strain, causing some departure from their predominantly concentric style.

From the constant orientation of axial planes and fold axes, it is concluded that a single episode of deformation would have been sufficient to produce the observed structure. As shown in Figure 3, although the fold axes are very nearly parallel to the contact between the jaspilite and the overlying greywacke, the axial planes of the folds appear to intersect the contact plane obliquely. The layering in the jaspilite near the contact lies parallel to it and is undisturbed; it is therefore concluded that the amplitude of the folding becomes attenuated near the contact and the model shown in Figure 5 is proposed. The sense of shearing is determined by the orientation of axial plains with respect to the main lithological boundary. Such a model explains the occurrence of intense folding in the jaspilite beds, which do not appear to be folded on a macroscopic scale.

Comparison of jaspilite with other iron formations

The Mount Ruker jaspilites resemble both the Lake Superior and Algoma type iron formations (Cross, 1970) in that they are almost entirely banded, with very little clastic iron ore material. The difference between these two types appears to be the different tectonic environments of the deposits; the environment of the Algoma type is eugeosynclinal and that of the Lake Superior type miogeosynclinal. The jaspilites on the eastern side of the embayment of Mount Ruker resemble the Lake Superior type in that they occur, associated with quartzites, close to an unconformity over crystalline basement rocks, and are interbedded with black slate and dolomitic shale. The occurrence of basic and andesitic volcanic rocks in the sequence suggest a transition to an Algoma type of environment. On the western side of the embayment the jaspilites lie within a monotonous sequence of greywacke and grey-green slate: a typical eugeosynclinal environment but for the absence of volcanic rocks. In most respects they resemble both the Archean and Proterozoic jaspilites of Western Australia (MacLeod, 1965; Evoy, 1970).

PLATE 8. Mount Ruker. Highly flattened concentric fold (Class 1C) in a siliceous layer. Note the extent to which ironstone has flowed to accommodate buckling in the siliceous layer.

PLATE 9. Disruption of highly flattened fold.

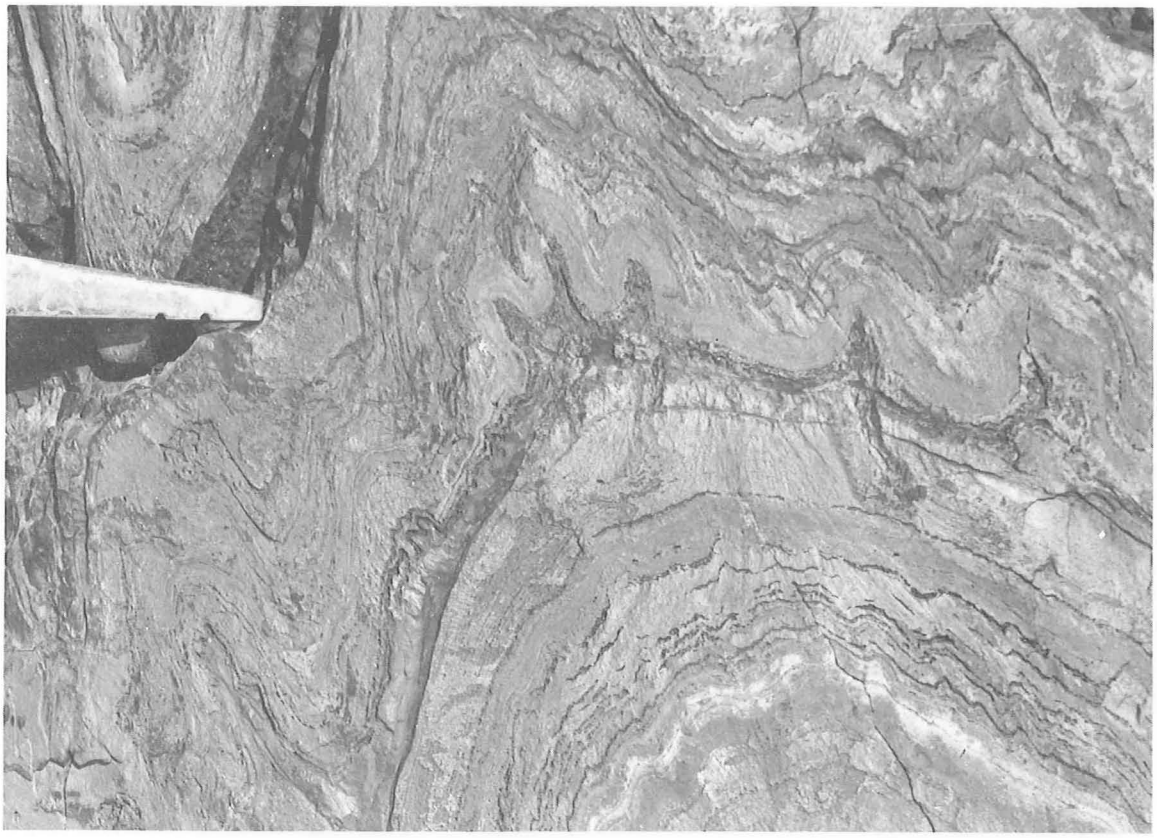

PLATE 10. Half-wave buckle folds in multilayered jaspilite.

PLATE 11. Fanning axial plane schistosity in a folded calcareous slaty band

MOUNT RUBIN (CUMPSTON MASSIF SHEET AREA, SS40-42/7)

A camp was made at the northern cliff face of Mount Rubin and an unsuccessful search was made for possible Cambrian fossils reported by G.C. Grikurov (pers. comm.). The locality is dominated by spectacularly folded, banded, chlorite-rich and chlorite-poor, sandy marls (Plate 12). Quartz sandstones are faulted against the marls in the west; Steeply dipping west-facing greywackes containing abundant flame structures abut against them in the east. Fold axes plunge at about 20° towards 300° and axial planes dip at about 60° to the southwest. The vergence in the folded marls, and the sense of faulting shown in Figure 6, suggest that relative movement between the two bodies of more competent rocks has been responsible for the folding in the marls sandwiched between them.

At glacier level, the quartz sandstones are folded into an overturned anticline and thrust against the marls at their western extremity (Fig. 6). The darker varieties of these quartz sandstones contain many clasts: pebbles and cobbles of granite, dolerite, chlorite schist, quartzite, and fine-grained marble are common. Farther to the west, dark grey quartz greywackes predominate.

Most of the sediments are of a deep-water character (suggesting geosynclinal origin), but volcanics are absent. The metamorphism reached biotite grade.

MOUNT NEWTON. NORTHERN PLATFORM (CUMPSTON MASSIF SHEET AREA, SS40-42/7)

The dominant rock type in the northern part of Mount Newton is melanocratic coarse-grained gneiss containing green hornblende, biotite, saussuritized sodic plagioclase, quartz, and scapolite. Hornblende grains in many rocks have ragged margins, and in the more strongly retrogressed rocks are locally surrounded by fine-grained brown biotite. The gneiss is generally

striped with quartz-plagioclase layers 0.5 to 1 cm thick; pinch-and-swell structures are developed in places (Plate 13). Later retrogression has resulted in the development of boudinage and augen structures, and has in places destroyed the striped layering. Within the hornblende-biotite gneiss are minor pelitic garnet-rich layers, and quartzite, marble, and calc-silicate bands up to several metres thick. The assemblage sillimanite + perthitic potash feldspar + quartz + albite antiperthite + garnet + reddish brown biotite places the early metamorphism in the uppermost amphibolite facies. (In the southern part of the mountain the metamorphic grade of this early event reached the threshold of the granulite facies). A specimen of strongly retrogressed pelitic gneiss collected in 1973 from the northwestern part of the mountain contains chloritoid and fine-grained patches of chlorite and sericite, probably after cordierite. The retrogression therefore occurred under greenschist facies pressure-temperature condition, probably at biotite grade.

Minor potash feldspar pegmatites and dolerite dykes intrude the hornblende-biotite gneiss. The pegmatites show a range of cataclastic deformation. Minor folds occur in the country rock adjacent to them but are rare elsewhere. The pegmatites were probably intruded between the two metamorphic events. Pods, up to several hundred metres across, of intrusive tholeiitic quartz-dolerite postdate the early metamorphism but have been affected by the retrogression; plagioclase (generally labradorite) is largely unaffected, but ferromagnesian minerals are mostly converted to uralite. In one specimen, pyroxenes are recrystallized to polygonal aggregates with both pigeonite and augite grains in varying orientations. The two forms of alteration may reflect varying availability of water during retrogression. The podiform shape of the dolerite bodies suggests boudinage (during the retrogressive metamorphism), of originally more continuous bodies of basic rock.

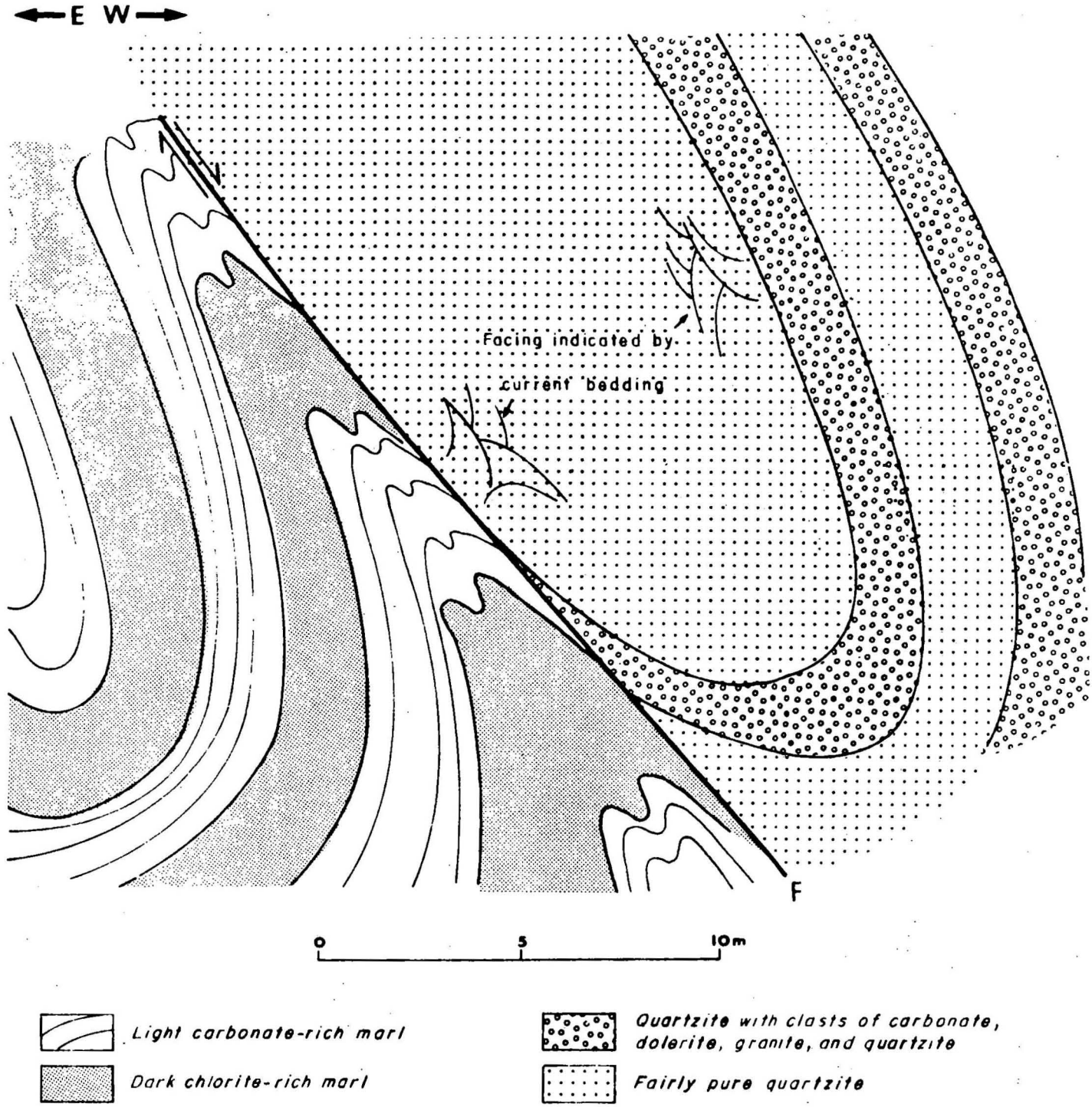

Fig.6-Northern cliff face of Mount Rubin: relationship between banded marls shown in Plate 12 and the more quartz-rich clastic rocks to the west

PLATE 12. Mount Rubin. Tight concentric folds in low-grade calcareous metasediments exposed in the northern cliff-face. Height of cliff 700 m.

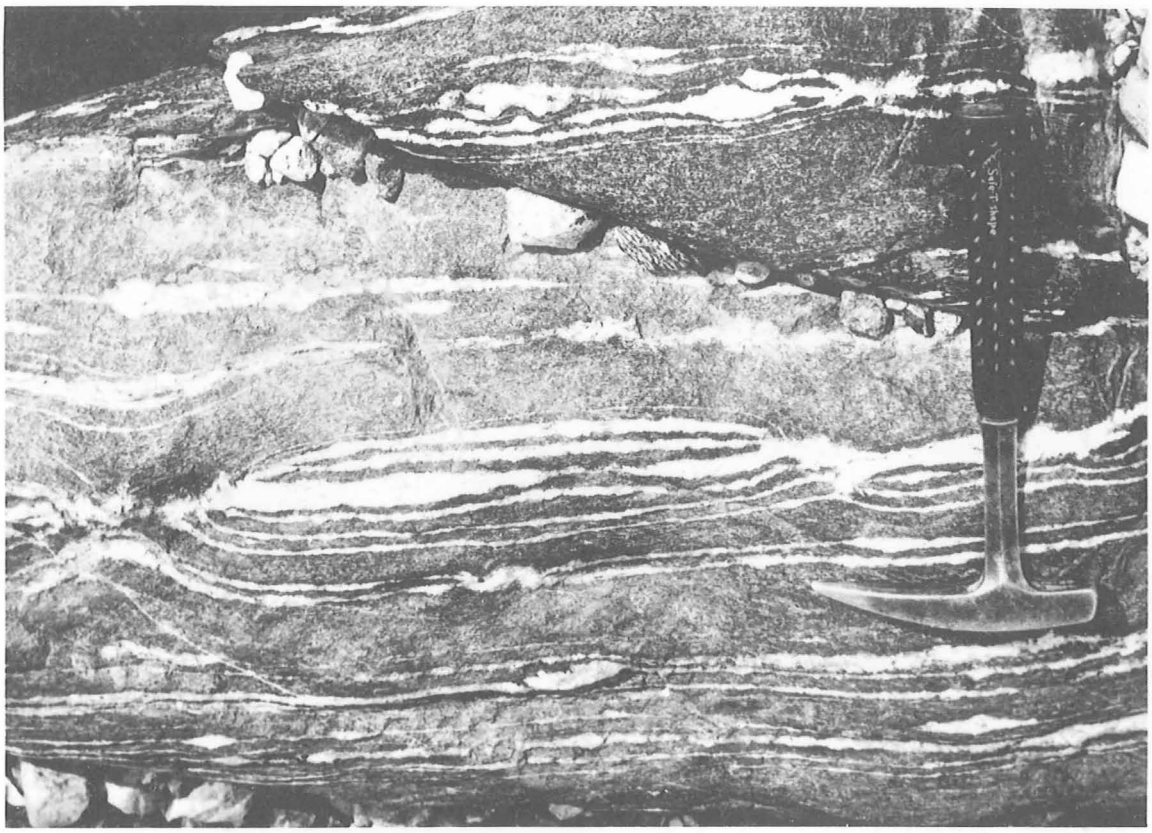

PLATE 13. Mount Newton. Pinch-and-swell structure in feldspathic bands in biotite amphibolite

SOUTH MAWSON ESCARPMENT (MAWSON ESCARPMENT SOUTH SHEET AREA, SS40-42/8)

The two southern headlands which were visited briefly by J.W. Sheraton in 1973 were mapped in greater detail in 1974. The southernmost headland, a low bench rising about 150 m above plateau level, appears to have only recently been exposed from ice cover. Glacial striae swing around from a westerly trend in the far south to a more northerly one in the west, parallel to the present sweep of glacial flow lines around the southern tip of the escarpment. The more northerly headland rises from about 300 m above the glacier in the south to a high plateau level (in the northern part of Fig. 7), about 1000 m above the glacier. The high plateau level is common to the rest of the escarpment.

In the northern part of the area shown in Figure 7, lower amphibolite facies psammopelitic metasediments dip at about 40° towards 030° - a slightly lower angle than their contact with the underlying quartzo-feldspathic gneiss, which dominates the central part of the area mapped. At the southern tip of the northern headland, similar psammo-pelites overlie the quartzo-feldspathic gneiss and dip at 45° towards 210°. The two outcrops of metasediments may belong to the limbs of an antiform, but there is little evidence beside the fact that they dip in opposite directions. On the southern headland, near-vertically dipping metasediments are sandwiched between the large body of quartzo-feldspathic gneiss and a finer-grained leucogneiss which forms the southern tip of the escarpment.

Quartzo-feldspathic gneiss

Coarse-grained well-foliated leucocratic gneiss forms the central part of Figure 7. A finer-grained more homogeneous and leucocratic variety forms the southern extremity of outcrop, and intrudes the metasediments as concordant layers up to 50 m thick and less common smaller cross-cutting

veins, which, although on a scale smaller than can be represented on the map, form a significant part of the rocks marked as metasediments in Figure 7.

In the central part of the area shown in Figure 7, the compositional layering in the metasediments, their contact with the coarse and fine leucogneisses, and the foliation in the gneisses, close to the contact are all parallel. (The northern leucogneiss-metasediment contact differs in that it cuts across the gross layering in the metasediments at a slight angle.) Several hundred metres north of the contact, however, the foliation in the coarse leucogneiss has a different orientation, possibly due to drag-folding associated with shearing near the contact. The foliation in the leucogneiss, best developed near the contact between the major rock units, is a fine penetrative compositional layering inherited from an early metamorphism. Within the darker layers, randomly oriented biotite and amphibole have crystallized in a later, lower amphibolite facies event.

A coarse-grained pegmatite interlayered between quartzo-feldspathic gneiss and metasediments on the southern headland is strongly deformed, with a foliation parallel to the lithological layering and penetrative regional foliation.

The quartzo-feldspathic gneisses appear, from the modal abundance of quartz, plagioclase, and microcline, to fall near the minimum melting composition in the system $NaAlSi_3O_8$-$KAlSi_3O_8$-SiO_2, suggesting a magmatic origin. They range in composition from granite - sensu stricto to adamellite. Plagioclase is albite or, less commonly, oligoclase. Obvious intrusive contacts between large bodies of coarse-grained leucogneiss are not found in the southern Mawson Escarpment and the possibility that these leucogneisses were originally an extensive sequence of acid volcanics cannot be ruled out.

PLATE 14. South Mawson Escarpment; northern headland of most southerly embayment. Interbanded pelitic metasediments (s) and leucogneiss (l), intruded by basic dykes (b). Massive leucogneiss on extreme left. Cliff height approximately 200 m.

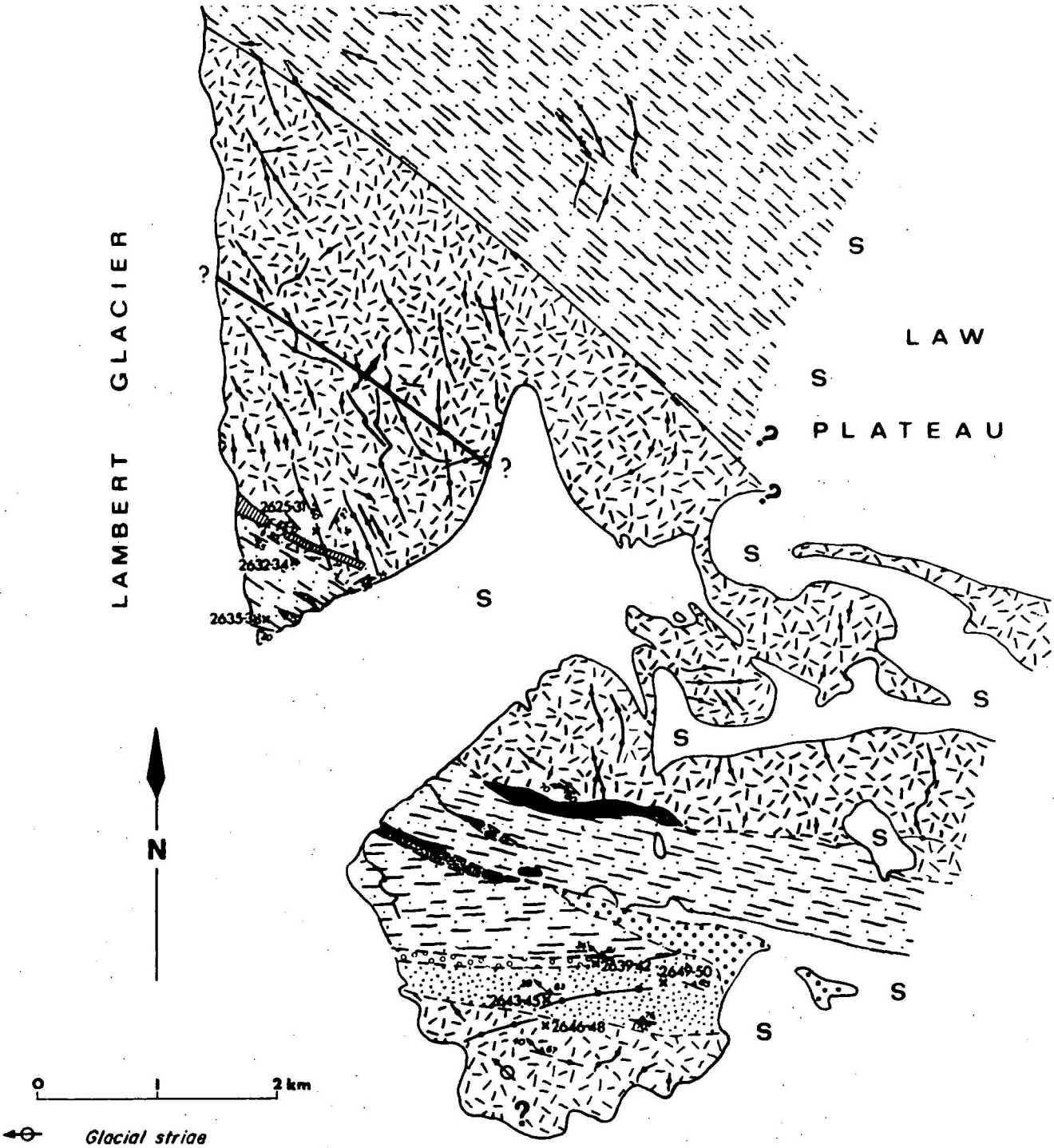

Glacial striae

Foliation with plunge of lineation

Strike and dip of bedding

Foliation with plunge of lineation

Amphibolite dyke

Dip of foliation

Pegmatite

Biotite-ferrohastingsite-bearing quartzo feldspathic gneiss

Calc-silicate gneiss

NOTE, map traced from air photo, MES tie run 3/056,057 and 058

Psammo-pelitic schist, garnet-bearing in places, containing rare staurolite and kyanite; calcareous in vicinity of marble. Minor concordant leucogneiss

Amphibolite

White tremolite marble

Impure quarzite, metapelitic rocks

Conglomerate

S *Permanent snow, ice*

Fig.7-Geological sketch map of the southern end of the Mawson Escarpment

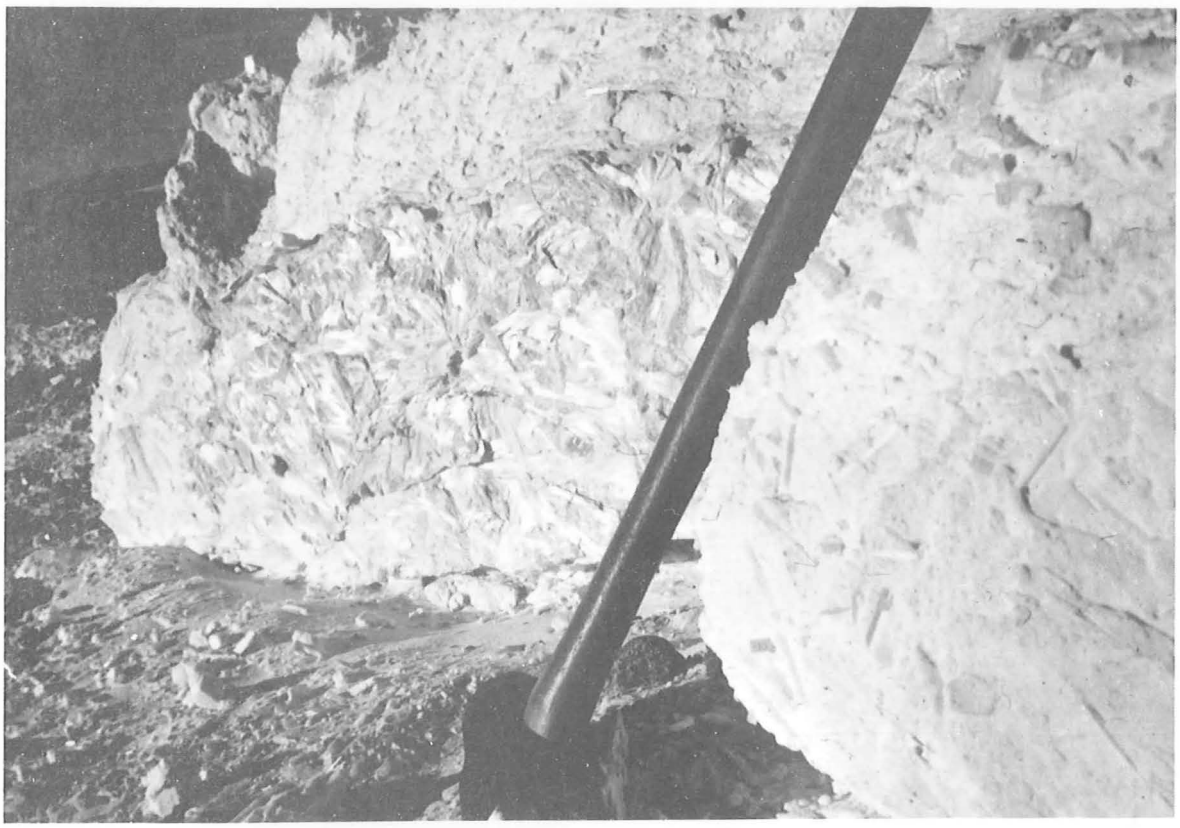

PLATES 15 and 16. South Mawson Escarpment. Outcrop of tremolite marble, with tremolite crystals up to 5 cm long. (The marble hummocks in the foreground and middle distance of Plate 15 are about 1 metre high.)

Ferromagnesian silicates are biotite, and deep blue-green hornblende with a very low optic axial angle. Similar hornblendes are common in K-feldspar-bearing rocks from the lower amphibolite and upper greenschist facies in the southern Prince Charle Mountains and elsewhere. Microprobe analyses of hornblendes with these optical characteristics (England, 1971) suggest that they are moderately potassic ferrohastingsites close to the composition $(Na, K)\ Ca_2\ (Fe, Mg)_4\ Fe^{3+}\ Al_2\ Si_6\ O_{22}\ (OH)_2$. The coarse-grained well-foliated leucogneiss and the aplitic type found within the metasediments have similar mineral assemblages.

Basic Dykes

Thoroughly amphibolitized basic dykes intrude both the quartzo-feldspathic gneiss and metasediments, although they are more common in the former. Amphibole grains have ragged outlines and are zoned, with actinolite cores and green hornblende rims. Small grains of opaque mineral are scattered through some actinolitic cores, but the hornblende rims are mostly free of inclusions. Zoned amphiboles with actinolitic cores are found in other metamorphic terrains (England, 1971). During progressive metamorphism, actinolite is transformed to hornblende by reaction with plagioclase and other phases. In rocks in which the reaction is incomplete, actinolitic cores may be preserved within amphibole grains. Fine-grained inclusions of iron oxides occur within actinolite cores because of the inability of actinolite to accommodate much iron (England, 1971). Their presence suggests that the actinolite formed as a result of transformation of a pre-existing more iron-rich phase such as pyroxene or hornblende. This phase might have been hornblende, as textures in the pelitic rocks (discussed in detail later) point to an early high-grade metamorphic event, which has been over-printed by the dominant lower amphibolite facies metamorphism. Abundant biotite in the amphibolites and the presence of a significant amount of microcline in one sample are ascribed to an influx during metamorphism of potassium from

the surrounding leucogneiss. The plagioclase is albite or oligoclase. A minor magmatic event, possibly correlated with the lower amphibolite facies retrograde metamorphism is indicated by the presence of small aplitic veins cutting a brecciated dyke in the northwestern part of Figure 7.

Metasediments

Psammo-pelitic schists are the most common metasedimentary rock types. However, quartzite and carbonate rocks were found at the southern part of the area shown in Figure 6. A wedge-shaped body of creamy white tremolite marble (Plates 15, 16) outcrops on the southern platform. This body is slightly discordant, a characteristic of marble which has undergone extreme plastic flow. Associated with the marble are grey biotite-actinolite schists and rusty-weathering impure marble containing rosettes to 15 cm across of pale green tremolite (J.W. Sheraton, pers. comm.). The calcareous schists closely resemble those from the northwestern part of Mount Menzies (J.W. Sheraton, pers. comm.). J.W. Sheraton (pers. comm.) has also suggested that the calcareous schists maybe younger than the early metamorphism. Concordant lenses of amphibolite of possible sedimentary origin occur within the sequence near the marble body.

Conglomerate bands (Plates 17 and 18), 0.5 to 3 m thick, consisting of rounded cobbles and pebbles of biotite-muscovite quartzite in a matrix of garnet-rich biotite-muscovite psammo-pelite occur a few hundred metres south of the marble. The conglomerate units are parallel to the regional schistosity. Long axes of deformed pebbles plunge at 34° the northwest, very nearly parallel to the penetrative lineation observed at many places on the southern platform. A considerable degree of flattening is evident in the conglomerates at some localities (Plate 18). Immediately south of the most prominent conglomerate band is a sequence of dirty quartzites containing minor biotite, epidote, and garnet; some layers are quite rich in garnet; some layers are quite rich in garnet. The quartzites are cut off in the south by a typical concordant fine-grained quartz-feldspathic gneiss of probable intrusive origin.

PLATE 17. South Mawson Escarpment. Highly deformed conglomerate band within amphibolite facies psammopelites. (Note pencil for scale)

The structure of the rocks making up the southern headland appears to be simple. The compositional layering dips steeply to the north, and a penetrative lineation plunges at a moderate angle to the west.

The psammo-pelitic rocks contain biotite and garnet, less commonly staurolite, and more rarely kyanite. Some of the garnet occurs as clots of small euhedra which appear to have replaced older large garnets. Staurolite and chlorite in places appear to have replaced garnet.

The textural relationships of garnet closely resemble those found near Edwards Pillar (Mount Stinear) and at Rooster Point, 20 km to the north of the area studied in detail, where staurolite has grown in fractures in early garnets. As the mg values $[Mg/(Mg + Fe + {}^{2+}Mn)]$ increase from garnet through staurolite to chlorite, and higher mg values are possible for garnet in high-grade terrains, replacement of garnet by staurolite and chlorite suggests a higher grade origin for the original garnet. Clots of small garnet euhedra, presumably after larger early garnets, suggest that the compositional field possible for garnet was previously larger. It is concluded, therefore, that early high-grade more-magnesian garnets broke down during retrogression; a small residue of more-Fe-Mn-Ca-rich garnet was left as the pyrope component was released for the formation of biotite and possibly chlorite. The original garnet-forming high-grade metamorphism may have been associated with the production of an anatectic melt, now represented by the fine-grained quartzofeldspathic gneiss layers.

Conclusions

(i) The boundary between the metasediments and the large body of coarse-grained quartzofeldspathic gneiss has at least been modified tectonically, and it may well have been faulting which originally brought the two into contact. It is also possible however, that the metasediments overlie the gneiss unconformably.

(ii) The bands of fine-grained gneiss within the metasediments have intrusive contacts.

(iii) Most, if not all, of the metasediments have been through an early high-grade event and are probably equivalent to the older basement rock.

(iv) The amphibolite dykes postdate the intrusive fine-grained leucogneiss, and cross-cut the boundary between metasediments and coarse-grained leucogneiss. It is not certain whether they were present during the high-grade metamorphism, which antedates the staurolite-grade event.

AUSTIN NUNATAK (GROVE MOUNTAINS SHEET AREA, SS40-42/8)

Austin Nunatak (72°55'12"S, 73°22'02"E) is a narrow east-west ridge with a very steep southern face but a more gently sloping northern side. The bulk of the outcrop (Fig. 8) is isoclinally folded, siliceous gneiss containing albite and microcline, with or without diopside, and biotite; its foliation and lithological layering dip at about 30° to the southwest. A small body of interbanded calc-silicate and finely banded microcline-rich gneiss occurs at the eastern end of the nunatak, where it underlies the quartz-rich rocks but is separated from them by a coarse-grained diopside-microcline pegmatite. The orientation of the structural elements of the banded gneiss is similar to that of the quartz-rich rocks.

The siliceous gneiss can be divided into more and less biotite-rich varieties (Plate 19), but the compositional difference between the two is small. Both varieties contain about 70 percent quartz, 5 to 10 percent albite, 5 to 10 percent microcline, a few percent of green clinopyroxene, biotite, and about 1 percent muscovite. The more mafic variety, which contains up to 10 percent of biotite and less diopside, occurs as raft-like bodies, 1 to 5 m thick and up to 20 m long, within the more-leucocratic gneiss. The ends of the bodies are whispy and poorly defined, but the upper

Fig.8-Geological sketch map of Austin Nunatak

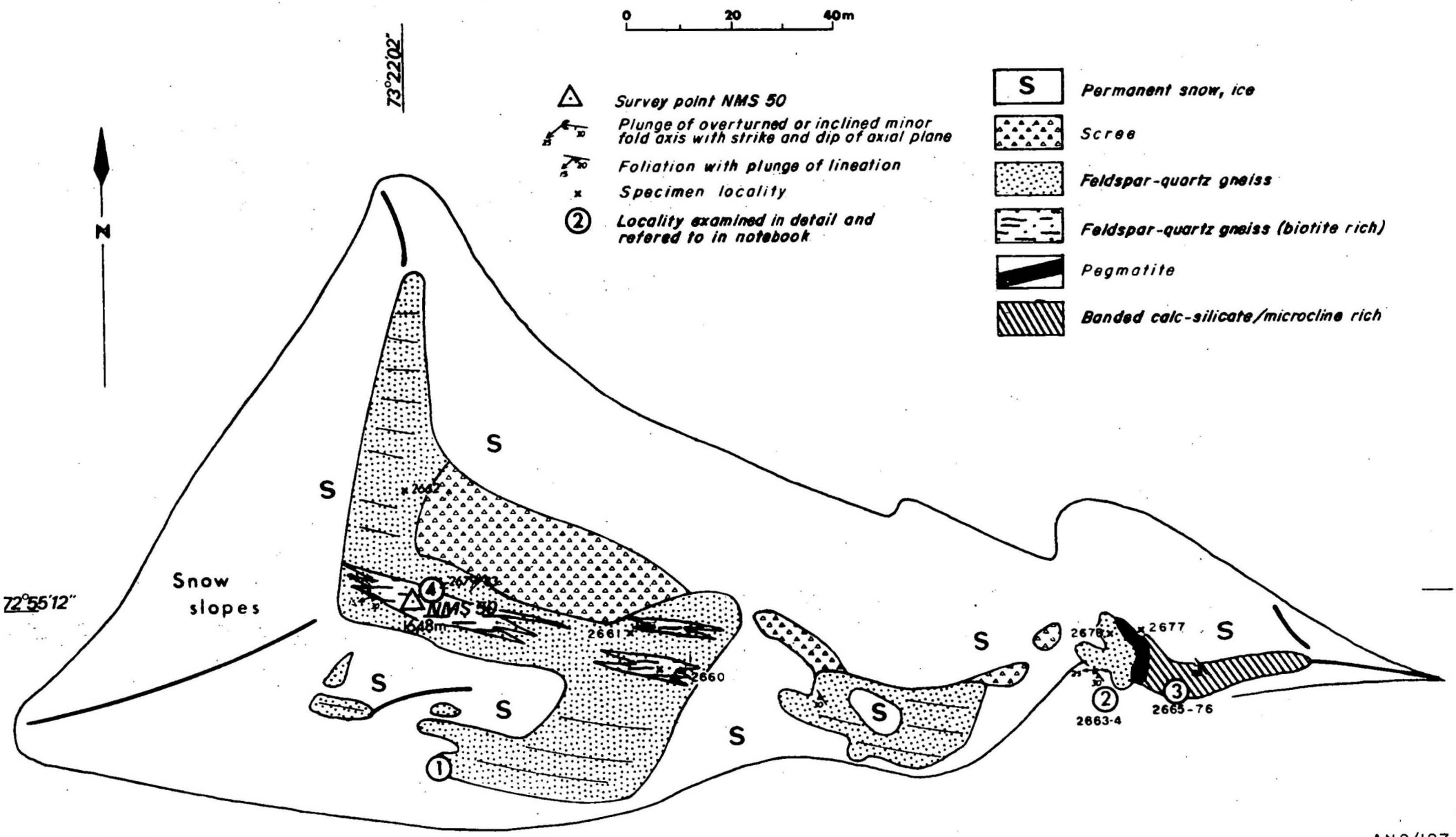

Record 1975/30

AN2/127

and lower contacts, which in places cut at a low angle across the foliation, are quite sharp (Plate 19).

Both types of gneiss include concordant lenses, up to 5 cm thick, of coarse-grained material, which give them a migmatitic appearance.

The more-mafic raft-like bodies, the leucocratic host rock, and the small lenses within both types all have high liquidi owing to their high quartz contents - probably close to 1000°C at moderate water pressure. Their solidi, however, are equally low (close to the granite minimum melting curve because quartz, albite, and microcline are all present). Under regional metamorphic conditions where temperature gradients are low, none of the rock types could have been liquid while any of the others was solid. A metamorphic or inherited origin is therefore required for the coarse-grained lenses and the occurrence of raft-like bodies.

A well-developed foliation (S_1) defined by a compositional layering of more and less mafic bands is more prominent in the dark gneisses. A second foliation (S_2), defined by the preferred orientation of biotite flakes, is parallel to S_1 except in the hinge regions of isoclinal folds, where it lies parallel to their axial planes (Plate 20). Cuspate folds occur in places (Plate 21). A well developed lineation defined by colour striping on S_1, and plunging at a shallow angle to the southwest, is exposed in some places.

The effects of retrogressive metamorphism are not as marked as in most parts of the southern Prince Charles Mountains. Clinopyroxene is locally replaced by actinolite, and secondary muscovite occurs in some rocks. Scapolite breakdown textures in the calc-silicate rocks are probably related to an influx of water and a consequent reduction in a_{CO_2}, which might have

occurred during the peak of metamorphism or during subsequent retrogression. Lack of diagnostic mineral assemblages precludes even a rough estimate of metamorphic grade. The quartz-rich rocks resemble those from Mount Twigg and are probably equivalent to the early high-grade rocks in the southern Prince Charles Mountains.

ACKNOWLEDGMENTS

This work was made possible by the very considerable efforts of the 1974 Prince Charles Mountains Party and the 1973 Mawson Wintering Party of the Australian National Antarctic Research Expeditions.

REFERENCES

ENGLAND, R.N. 1971 - Progressive metamorphism of amphibolites from the Cloncurry and Petermann Ranges areas. Bur. Miner. Resour. Aust. Rec. 1971/109 (unpubl.).

EVOY, E.F. 1970 - Iron ore deposits of Australia, New Zealand and New Caledonia. UN Dept Economic & Social Affairs, Survey of World Iron Ore Resources.

GROSS, G.A. 1970 - Nature and occurrence of iron ore deposits. UN Dept Economic & Social Affairs, Survey of World Iron Ore Resources.

MACLEOD, W.N. 1965 - Banded iron formations of Western Australia. 8th Comm. Min. Metall. Congr., 1.

RAMSAY, J.G. 1967 - Folding and fracturing of rocks. New York, McGraw-Hill.

SOLOVIEV, D.S. 1972 - Geological structure of the mountain fringe of Lambert Glacier and Amery Ice Shelf. In ADIE, R.J. (Ed.) - Antarctic geology and geophysics. Universitetsforlaget.

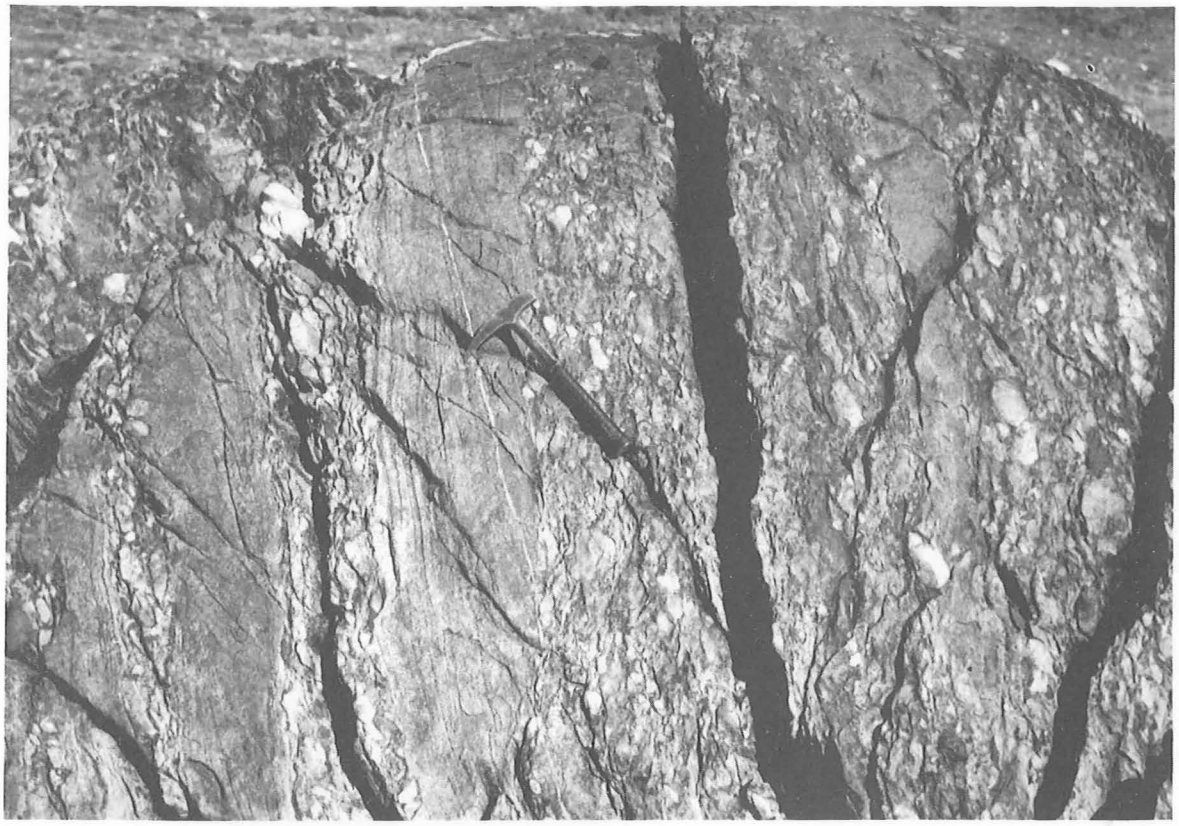

PLATE 18. South Mawson Escarpment. Relatively undeformed steeply dipping conglomerate beds.

PLATE 19. Austin Nunatak. Biotite-rich and biotite-poor siliceous gneiss. Coarse-grained layers within the more mafic material are 1 - 5 cm thick.

PLATE 20. Austin Nunatak. Axial plane schistosity, S_2 (defined by preferred orientation of biotite) developed in a mesoscopic fold in banded siliceous gneiss. (Note hammer head at bottom left for scale).

PLATE 21. Austin Nunatak. Cuspate flexural flow folding in banded siliceous biotite gneiss.

APPENDIX: MINERAL ASSEMBLAGES OF SPECIMENS COLLECTED

Aerial photographs: Run 9/64 Mount Ruker (Cumpston Massif Sheet area, SS40-42/7).

Specimen	Assemblage	Comments
74282505	Chlorite + quartz + opaque	BLACK SLATE
74282506	Actinolite + epidote + quartz + sphene + opaque	ALTERED BASIC ROCK Epidote replacing plagioclase
74282507	Green muscovite + quartz	QUARTZITE
74282508	An_{33} + K-feldspar + quartz + biotite (secondary) + magnetite + calcite + muscovite	ANDESITE
74282509	Dolomite + muscovite + chlorite + albite + quartz + opaque + tourmaline	CALCAREOUS SCHIST
74282510	Magnetite + quartz + biotite + calcite	JASPILITE
74282511	Epidote + calcite + chlorite + actinolite + biotite + sphene + albite + quartz	ALTERED BASIC
74282512	Chlorite + carbonate + quartz + opaque	BLACK SLATE
74282513	Magnetite + riebeckite + brown biotite + carbonate + quartz	JASPILITE
74282514	Magnetite + riebeckite + minnesotaite? + carbonate + quartz	JASPILITE
74282515	Actinolite + saussurite + sphene + quartz	ALTERED BASIC
74282516A	Magnetite + riebeckite + quartz	JASPILITE
74282516B	Quartz + carbonate + chlorite + opaque + biotite	METAGREYWACKE
74282606	Biotite + quartz + chlorite opaque	BLACK SLATE
74282607	Biotite + quartz + muscovite + chlorite	BLACK SLATE
74282611	Biotite + chlorite + muscovite + quartz	BLACK SLATE
74282614	Carbonate + biotite + muscovite + zoned plagioclase + quartz	CALCAREOUS PHYLLITE
74282617	Biotite + chlorite + quartz + carbonate + opaque	BLACK SLATE
74282619	Magnetite + quartz + biotite + stilpnomelane + chlorite + carbonate	JASPILITE
74282622	Magnetite + quartz + carbonate + biotite + stilpnomelane	JASPILITE

Specimen	Assemblage	Comments
74282530	Garnet + quartz + deep blue-green hornblende + green (and brown) biotite	Garnet interstitial to quartz
74282531	Quartz + saussuritized albite + orthoclase perthite + biotite	PEGMATITE
74282532	Albite + microcline + quartz + biotite	LEUCOGNEISS

Aerial photograph: Run 6/88 Mount Rubin (Cumpston Massif Sheet area, SS40-42/7).

Specimen	Assemblage	Comments
74282533	Quartz + albite + microcline + sericite + carbonate + opaque	GRANODIORITE CLAST
74282534	Quartz + clouded plagioclase + microcline + carbonate + biotite	ADAMELLITE CLAST
74282623	Muscovite + biotite + carbonate + quartz	BIOTITE SCHIST
74282624	Quartz + albite + biotite + muscovite + chlorite + opaque + rutile	QUARTZITE

Aerial photograph: Run 13/247 Mount Newton (Cumpston Massif Sheet area, SS40-42/7).

Specimen	Assemblage	Comments
74282520	Biotite + oligoclase + quartz + tourmaline	MAFIC GNEISS Biotite partly retrogressed
74282521	An_{51} + actinolite + sphene + quartz + biotite + opaque	QUARTZ DOLERITE Uralite replacing pyroxene
74282522	Green hornblende + scapolite + andesine + quartz + biotite	MAFIC GNEISS Partly retrogressed
74282523	Garnet + An_{10} + quartz + biotite + opaque	GARNET GNEISS Some minerals deformed
74282524	Green hornblende + saussuritized plagioclase + biotite + quartz	MAFIC GNEISS Hornblende rimmed by fine-grained biotite
74282525	Green hornblende + saussuritized plagioclase + biotite + quartz	MAFIC GNEISS Hornblende rimmed by fine-grained biotite
74282526	An_{48} + augite + pigeonite + quartz + opaque	QUARTZ DOLERITE Pyroxenes recrystallized

Specimen	Assemblage	Comments
74282527	Mesoperthite + sillimanite + quartz + garnet + biotite + albite antiperthite	PELITIC GNEISS Upper amphibolite facies
74282528	Chlorite + actinolite + biotite + opaque	STRONGLY ALTERED DOLERITE
74282529	Scapolite + sericitized oligoclase + quartz + muscovite	PEGMATITE Scapolite sericitized Me_{30}

Aerial photograph: Run 3/57 South Mawson Escarpment (Mawson Escarpment South Sheet Area, SS40-42/8)

Specimen	Assemblage	Comments
74282535	Garnet + biotite + microcline + albite + quartz	PSAMMO-PELITE
74282537	Biotite + microcline + albite + opaque + muscovite + quartz	PSAMMO-PELITE
74282538	Microcline + albite + quartz + biotite	QUARTZO-FELDSPATHIC ORTHOGNEISS
74282539	Microcline + albite + muscovite + quartz + opaque	PEGMATITE
74282540	Garnet + quartz + biotite + muscovite + oligoclase	PSAMMA-PELITE Muscovite may be relict
74282541	Microcline + albite + quartz + biotite + ferrohastingsite	QUARTZO-FELDSPATHIC ORTHOGNEISS Segregation?
74282542	Microcline + oligoclase + biotite + opaque + allanite?	QUARTZO-FELDSPATHIC ORTHOGNEISS
74282543	Ferrohastingsite + biotite + garnet + albite	AMPHIBOLITE
74282544	Zoned hornblende + zoned moderately sodic plagioclase + microcline + quartz + biotite	AMPHIBOLITE
74282545	Tremolite + biotite	CALC-SILICATE SCHIST
74282546	Green hornblende + oligoclase + quartz + biotite	CALC-SILICATE SCHIST
74282547	Tremolite + green biotite	CALC-SILICATE SCHIST
74282548	Garnet + biotite + quartz + chlorite + muscovite	PSAMMITE
74282549	Microcline + oligoclase + biotite + opaque	APLITE
74282550	Microcline + albite + quartz + opaque + biotite	APLITE
74282551	Microcline + oligoclase + ferrohastingsite	QUARTZO-FELDSPATHIC GNEISS

Specimen	Assemblage	Comments
74282552	Quartz + oligoclase + magnetite + biotite + microcline + sphene	QUARTZO-FELDSPATHIC GNEISS (quartz-rich)
74282553	Zoned amphibole + biotite + opaque + sodic plagioclase + apatite	AMPHIBOLITE Actinolite cores crowded with opaques
74282554	Staurolite + kyanite + muscovite + quartz + chlorite + magnetite	PELITIC SCHIST
74282555	Garnet + biotite + muscovite + chlorite + quartz + opaques	PELITIC SCHIST Dark pleochroic rims, haloes around veins suggest presence of radioactive elements at grain boundaries
74282556	Quartz + oligoclase + biotite + microcline + secondary chlorite	QUARTZO-FELDSPATHIC ORTHOGNEISS
74282557	Garnet + biotite + muscovite + chlorite + oligoclase + opaque	PSAMMO-PELITE

Aerial photograph: Tie run 3/58 South Mawson Escarpment (Mawson Escarpment South, SS40-42/8)

Specimen	Assemblage	Comments
74282625	Microcline + albite + quartz + biotite + opaque + sphene	QUARTZO-FELDSPATHIC ORTHOGNEISS
74282626	Actinolite + biotite + chlorite + carbonate + opaques	ACTINOLITE SCHIST Retrogressed and altered amphibolite
74282627	Hornblende + biotite + quartz + albite + opaque	AMPHIBOLITE
74282628	Albite + microcline + quartz + biotite	QUARTZO-FELDSPATHIC ORTHOGNEISS
74282629	Oligoclase + microcline + biotite	QUARTZO-FELDSPATHIC ORTHOGNEISS
74282630	Albite + microcline + biotite + muscovite + quartz	QUARTZO-FELDSPATHIC ORTHOGNEISS
74282631	Oligoclase + quartz + biotite + muscovite	QUARTZO-FELDSPATHIC ORTHOGNEISS
74282632	Ferrohastingsite + oligoclase + microcline + biotite + quartz + opaque + sphene	QUARTZO-FELDSPATHIC ORTHOGNEISS

Specimen	Assemblage	Comments
74282633	Albite + microcline + ferrohastingsite + quartz + biotite + muscovite	QUARTZO-FELDSPATHIC ORTHOGNEISS WITH PEGMATITE
74282634	Oligoclase + microcline + ferrohastingsite + biotite + sphene + quartz + opaque	QUARTZO-FELDSPATHIC ORTHOGNEISS WITH PEGMATITE
74282635	Garnet + biotite + muscovite + quartz + albite + microcline + hornblende + apatite + opaque + chlorite	QUARTZO-FELDSPATHIC ORTHOGNEISS
74282636	Biotite + actinolite + opaque	CALC-SILICATE GNEISS
74282637	Staurolite + garnet + albite + quartz + biotite + chlorite	PELITIC SCHIST
74282638	Blue-green hornblende + biotite + quartz + chlorite + opaques	AMPHIBOLITE
74282639	Biotite + muscovite + quartz (pebbles) + garnet + biotite + muscovite + quartz (matrix)	CONGLOMERATE
74282640	Garnet + biotite + muscovite + quartz + opaques	CONGLOMERATE Garnet recrystallized
74282641	Muscovite + biotite + garnet + quartz	CONGLOMERATE
74282642	Muscovite + biotite + garnet + quartz + chlorite	PSAMMITIC LAYER IN CONGLOMERATE
74282643	Biotite + hornblende + quartz + albite + epidote + sphene	AMPHIBOLITE
74282644	Garnet + biotite + quartz	PELITIC GNEISS
74282645	Quartz + garnet + epidote + biotite	IMPURE QUARTZITE
74282646	Quartz + microcline + oligoclase + ferrohastingsite + biotite + opaque + sphene	QUARTZO-FELDSPATHIC ORTHOGNEISS
74282647	Quartz + microcline + oligoclase + ferrohastingsite + biotite + opaque + sphene	QUARTZO-FELDSPATHIC ORTHOGNEISS
74282649	Quartz + plagioclase (zoned from andesine to albite) + biotite + muscovite	SILICEOUS CONGLOMERATE
74282650	Quartz + biotite + muscovite + microcline + (seriditized) albite	PSAMMITE

Austin Nunatak (Grove Mountains Sheet area, SS43-45/1).

Specimen	Assemblage	Comments
74282660	Quartz + microcline + andesine + biotite opaque + sericite	SILICEOUS GNEISS (RAFT)
74282661	Quartz + microcline + sericitized plagioclase + calcite + sericite + opaque	CALCAREOUS QUARTZITE
74282662	Quartz + calcite + biotite + green clino-pyroxene + oligoclase + apatite + opaque	CALCAREOUS QUARTZITE
74282663	Quartz + microcline + biotite +sericite + sericitized plagioclase	SILICEOUS GNEISS
74282664	Quartz + oligoclase + microcline + biotite + sericite + green clinopyroxene	SILICEOUS GNEISS (RAFT)
74282665	Green clinopyroxene + calcite + epidote + apatite + brownish garnet + albite + scapolite + microcline + quartz	CALC-SILICATE GNEISS
7428266	Oligoclase + quartz + biotite + sericite	OLIGOCLASE GNEISS
74282667	Microcline + sericitized plagioclase + green clinopyroxene + quartz + opaques + sericite	MICROCLINE-RICH GNEISS
74282668	Microcline + quartz + oligoclase + green clinopyroxene + biotite + sphene + opaque + sericite	MICROCLINE-RICH GNEISS
74282669	Quartz + scapolite + calcite + brownish garnet + oligoclase + epidote + sphene + sericite	CALCAREOUS QUARTZITE
74282670	Quartz + microcline + green clinopyroxene + oligoclase + sphene + carbonate	SILICEOUS GNEISS WITH MICROCLINE-RICH BANDS
74282671	Microcline + oligoclase + quartz + sphene + green clinopyroxene + opaque	MICROCLINE-RICH GNEISS
74282672	Calcite + brownish garnet + oligoclase + microcline + quartz + green clinopyroxene + sphene + sericite + biotite	CALC-SILICATE GNEISS
74282673	Microcline + albite + quartz + green clino-pyroxene + opaque + sphene	MICROCLINE-RICH GNEISS
74282674	Green clinopyroxene + microcline + albite + brown garnet + sphene + opaques	MICROCLINE-RICH GNEISS
74282676	Scapolite + garnet + epidote + calcite + oligoclase + quartz + microcline	CALC-SILICATE GNEISS
74282677	Albite + microcline + quartz + green clino-pyroxene + sericite + opaque	PEGMATITE
74282678	Quartz + microcline + albite + sericite + opaque	SILICEOUS GNEISS

Specimen	Assemblage	Comments
74282679	Quartz + microcline + biotite + sericitized plagioclase + actinolite + opaque + chlorite + sericite	SILICEOUS GNEISS
74282680	Quartz + microcline + biotite + oligoclase + sericite + actinolite + opaque	SILICEOUS GNEISS
74282681	Quartz + microcline + oligoclase + sericite + opaque	SILICEOUS GNEISS
74282681	Quartz + microcline + oligoclase + sericite + opaque	SILICEOUS GNEISS
74282682	Quartz + microcline + oligoclase + sericite + opaque	SILICEOUS GNEISS
74282683	Quartz + microcline + oligoclase + sericite + opaque	SILICEOUS GNEISS